THE JOURNAL OF BIOLOGICAL CHEMISTRY VOL. 287, NO. 2, pp. 1242–1251, January 6, 2012


# Long Glucocorticoid-induced Leucine Zipper (L-GILZ) Protein Interacts with Ras Protein Pathway and Contributes to Spermatogenesis Control*[S]

Received for publication, October 21, 2011, and in revised form, November 18, 2011 Published, JBC Papers in Press, November 22, 2011, DOI 10.1074/jbc.M111.316372

**Stefano Bruscoli[‡], Enrico Velardi[‡], Moises Di Sante[‡], Oxana Bereshchenko[‡], Alessandra Venanzi[‡], Maddalena Coppo[‡], Valeria Berno[§], Maria Grazia Mameli[¶], Renato Colella[¶], Antonio Cavaliere[¶], and Carlo Riccardi[‡1]**

*From the [‡]Department of Clinical and Experimental Medicine, Section of Pharmacology, Toxicology, and Chemotherapy, and [¶]Institute of Pathological Anatomy and Histology, Medical School, University of Perugia, Via del Giochetto, 06122 Perugia, Italy and the [§]Mouse Biology Unit, European Molecular Biology Laboratory, Campus A. Buzzati-Traverso, 00015 Rome, Italy*

**Background:** Understanding how spermatogenesis occurs in mammals is not yet fully understood.
**Results:** L-GILZ deficiency in germ cells leads to complete loss of germ cell lineage resulting in male sterility.
**Conclusion:** Our study identifies L-GILZ as an important factor for spermatogenesis.
**Significance:** Identification of genes critical for maintenance of spermatogenesis is pivotal for diagnosis and treatment of male infertility.

**Correct function of spermatogonia is critical for the maintenance of spermatogenesis throughout life, but the cellular pathways regulating undifferentiated spermatogonia proliferation, differentiation, and survival are only partially known. We show here that long glucocorticoid-induced leucine zipper (L-GILZ) is highly expressed in spermatogonia and primary spermatocytes and controls spermatogenesis. *Gilz* deficiency in knockout (*gilz* KO) mice leads to a complete loss of germ cell lineage within first cycles of spermatogenesis, resulting in male sterility. Spermatogenesis failure is intrinsic to germ cells and is associated with increased proliferation and aberrant differentiation of undifferentiated spermatogonia and with hyperactivity of Ras signaling pathway as indicated by an increase of ERK and Akt phosphorylation. Spermatogonia differentiation does not proceed beyond the prophase of the first meiotic division due to massive apoptosis associated with accumulation of unrepaired chromosomal damage. These results identify L-GILZ as a novel important factor for undifferentiated spermatogonia function and spermatogenesis.**

Spermatogenesis is a tightly controlled process of germ cell maturation programmed to produce spermatozoa through life (1). The generation and maintenance of the germ cell lineage occur within the seminiferous tubules of the testis where the processes of spermatogonia proliferation and differentiation take place (1, 2). The molecular mechanisms underlying the function of undifferentiated spermatogonia have not been elucidated largely due to the lack of specific biologic markers. The undifferentiated spermatogonia population contains the spermatogonial stem cells (SSCs),[2] which are the adult stem cells of germ cell lineage. An appropriate equilibrium between SSC self-renewal, proliferation, and differentiation is necessary to maintain spermatogenesis and male fertility. Previous studies have implicated several genes in the regulation of undifferentiated spermatogonia function, but factors influencing their proliferation and differentiation to mature germ cells have not been fully defined (3–8).

The Ras signaling pathway is important in regulating cell proliferation, survival, and differentiation (9). Ras interacts with and activates several effectors which in turn trigger a multitude of signaling pathways (10). Raf and PI3K, the best characterized Ras effectors, activate respectively MEK/ERK kinase and Akt/PKB serine/threonine kinase (Akt) cascades (11) and cooperate in regulating cell death and proliferation (12–15). Moreover, Ras activity correlates with ERK and Akt phosphorylation and cyclin D1 expression. Notably, Ras signal transduction is controlled by several proteins which, by enhancing or disrupting physical interactions between pathway components, efficiently up- and down-regulate the signal (16, 17). It is well established that such control mechanisms, based on protein-to-protein interaction, serve to maintain normal cell growth rate and function (18–21).

Glucocorticoid-induced leucine zipper (GILZ) was initially described as a regulator of the immune response and an important player of the anti-inflammatory and immunomodulatory effects of glucocorticoids. Glucocorticoid effects are in part due to the GILZ-mediated modulation of cell proliferation and differentiation (22–25). In particular, we have shown that GILZ directly binds Ras and inhibits downstream MAPK/ERK Ras-dependent signals, thus functioning as a physiological brake on cell proliferation (26). Moreover, we have shown that this

* This work was supported by Associazione Italiana per la Ricerca sul Cancro (AIRC), Milan, Italy (to C. R.).
[S] This article contains supplemental Figs. S1–S4, Tables S1 and S2, Materials and Methods, and additional references.
[1] To whom correspondence should be addressed: Dept. of Clinical and Experimental Medicine, Section of Pharmacology, University of Perugia, Via del Giochetto, 06100 Perugia, Italy. Tel.: 39-075-5857467; Fax: 39-075-5857405; E-mail: riccardi@unipg.it.

[2] The abbreviations used are: SSC, spermatogonial stem cell; α6-int, α6-integrin; dpp, days postpartum; GILZ, glucocorticoid-induced leucine zipper; L-GILZ, long GILZ; GSEA, Gene Set Enrichment Analysis; LH, luteinic hormone; qPCR, quantitative PCR; PLZF, promyelocytic leukaemia zinc finger.

inhibitory effect is associated with decreased ERK, Akt, and Rb phosphorylation, and cyclin D1 expression (26, 27).

The GILZ locus gene is characterized by two main isoforms, GILZ and a longer isoform, long GILZ (L-GILZ), that are expressed differentially in various tissues (28). We show here that L-GILZ is the only isoform expressed in testis. Using *gilz* knock-out (*gilz* KO) mice, we demonstrate that L-GILZ is important for spermatogenesis. *Gilz* deletion in germ cells results in eradication of germ cell lineage, associated with hyperactivation of Ras signaling, increased spermatogonia proliferation at the premeiotic phase, deregulated meiotic gene expression, and massive apoptosis in meiosis.

## EXPERIMENTAL PROCEDURES

*Generation of Gilz KO Mice*—Animal care was in compliance with regulations in Italy (Ministerial Decree 116192), Europe (O.J. of European Community 358/1 December 18, 1986), and the United States (Animal Welfare Assurance No. A5594-01, Department of Health and Human Services, Washington, DC). For genotyping, genomic DNA was isolated from mice tails, and genotypes were determined by Southern blot analysis. 15–20 $\mu$g of DNA was digested with KpnI or HindIII and separated in a 0.8% agarose gel. The DNA was transferred to a GeneScreen Plus membrane (PerkinElmer Life Sciences) and hybridized with 5′ or 3′ probes. The 5′ probe hybridizes to 5.0-kb (WT) and 7-kb (targeted) HindIII fragments. The 3′ probe hybridizes to 12.4-kb (WT) and 8.4-kb (targeted) KpnI fragments.

*Histology*—Mouse testes at various stages were collected and fixed for 24 h in 10% buffered formalin and embedded in paraffin wax. Semiserial sections were stained with H&E or used for immunohistochemistry. Dewaxed and rehydrated sections of WT and *gilz* KO testes at the indicated time points were incubated with specific antibodies for L-GILZ (eBioscience), PLZF (Calbiochem), GATA-1 (Santa Cruz Biotechnology), TRA98 (BioAcademia), cyclin D1 (Santa Cruz Biotechnology), and γH2AX (Upstate). Rat IgG2a K isotype control was purchased from BD Biosciences. A full automated staining system (Vision BioSystems Bond Max) was used for the immunohistochemical staining using a biotin-free polymeric HRP linker antibody conjugate system (Bond Polymer Defined Detection; Vision BioSystems Ltd.). The number of positive cells/seminiferous tubule was counted for six individual animals and average values and standard deviation determined. At least 60 seminiferous tubules were counted per testis. Digital images were acquired with an Olympus BX51 microscope equipped with a Leica EC3 camera (Leica) and analyzed with LAS EZ software (Leica).

*Cell Staining and Flow Cytometry*—Analysis of testis cell suspensions was obtained from 7-days postpartum (dpp) testes by enzymatic digestion with type I collagenase (Sigma), filtered through a 70-$\mu$m nylon mesh, and incubated in cell dissociation buffer (Invitrogen) for 25 min at 32 °C. After centrifugation, cells were incubated with anti-integrin-$\alpha$6 ($\alpha$6-int; eBioscience), anti-c-Kit (eBioscience), or phosphorylated Ser-473 Akt (pAkt; Cell Signaling) antibodies for 15 min at room temperature in PBS and 2% FCS and washed twice with excess of PBS and 2% FCS.

*Proliferation BrdU Assay*—Cell proliferation was measured by BrdU incorporation (Roche Applied Science). Cells were plated at $10^6$ cells/well and treated with 0.2 $\mu$M wortmannin (Sigma) for 6 h. BrdU was added during last 2 h. Cells were stained with surface markers for 15 min, washed, and fixed in 2% paraformaldehyde. Incorporated BrdU was immunodetected using FITC BrdU Flow Kit (BD Biosciences). Flow cytometry experiments were performed using a one laser standard configuration FACS Canto (BD Biosciences). Data were analyzed using FlowJo software (Tree Star).

*Whole Mount Immunostaining*—Tubules were removed from the tunica albuginea from WT and *gilz* KO testis at 7, 10, 14, 25, and 35 dpp ($n = 5$) and fixed with 4% paraformaldehyde at 4 °C. Samples were incubated overnight at 4 °C with primary antibodies with PBS, 0.1% Triton X-100, 1% BSA, 5% donkey serum against PLZF and GILZ. After washing, samples were incubated with anti-mouse Alexa Fluor 488 or anti-rat Alexa Fluor 568 secondary Abs (Invitrogen). Successively, tubules were mounted on slides with Vectashield (Vector Laboratories). Nuclei were counterstained with Hoechst 33342. Confocal photomicrographs were acquired with a Leica TCS SP2 (Leica) equipped with three laser lines (argon 488, 543, 633 nm). Each channel was acquired separately using specific laser lines to avoid bleed-through of the fluorochromes. Photomicrographs were acquired with LAS AF Software (Leica) at 1024 × 1024 or 2048 × 2048 pixels. Values for positive staining cells were measured using the National Institutes of Health software program ImageJ.

*Quantitative Real Time PCR Analysis*—Total RNA was extracted using TRIzol (Invitrogen). RT-PCR was done using QuantiTect Reverse Transcription (Qiagen). PCR analyses were done with the primers shown in supplemental Table S2. PCR was performed in a final volume of 20 $\mu$l containing 0,02 $\mu$M cDNA, 0.5 $\mu$M sense and antisense primers, 1.5 mM $MgCl_2$, and 1 unit of platinum TaqDNA polymerase (Invitrogen). The PCR was done according to the manufacturer's instructions. The PCR products were electrophoresed on a 2% agarose gels in the presence of ethidium bromide. Real-Time quantitative PCR (qPCR) analysis was performed in Applied Biosystems Real Time PCR machine (AB7300) using Power SYBR Green PCR Master Mix (Applied Biosystems). Relative amounts of L-GILZ and other mRNAs analyzed (supplemental Table S2) were calculated by the Comparative ΔΔC(t) method.

*Cell Transfection and Immunoprecipitation*—HEK293 cells were transfected using Lipofectamine 2000 (Invitrogen) according to the manufacturer's instructions, with pcDNA3.1-FLAG-L-GILZ and pCMVTag-H-Ras-Myc. 24 h after transfection, whole cell extracts were prepared, and immunoprecipitations were performed with anti-FLAG M2 beads (Sigma). Inputs and immunoprecipitated proteins were separated by SDS-PAGE and analyzed by Western blotting. Exogenous expression of transfected proteins was detected by primary Abs recognizing FLAG peptide (Sigma) and Myc peptide (Invitrogen).

*Western Blotting*—Total protein extracts in radioimmunoprecipitation assay buffer were separated by SDS-PAGE, transferred to the PVDF membrane, and immunoblotted using the primary antibodies against GILZ (Santa Cruz Biotechnology), ERK1/2 and phospho-ERK1/2, Akt and phospho-AKT Ser-473

(Cell Signaling), and β-tubulin (Sigma-Aldrich); signal was revealed using secondary HRP-conjugated antibodies (Thermo Scientific) and the ECL visualization system (Amersham Biosciences). Western blot films were scanned, and band signal intensities were determined using Scion Image software (Scion Corporation). Expression levels were normalized to β-tubulin expression.

*Gene Expression Profiling*—The experiment was performed using 12 Affymetrix GeneChip Human Mouse ST 1.0 arrays. The aim of the analysis was to compare gene expression profiling of 7-dpp testes from WT and *gilz* KO mice. Total RNAs were purified from 7-dpp testes from WT and *gilz* KO littermates using TRIzol (Invitrogen). 18 samples were pooled in six groups, each made of three biological replicates. The two experimental groups were: WT 7 dpp; KO 7 dpp. Differentially expressed genes were identified using Partek Genomic Suite 6.4 software. ANOVA was performed and differentially expressed genes filtering for a false discovery rate $< 0.05$. A $p$ value $< 0.05$ and -fold change $> 1.5$ (in modulus) were used to filter.

Additional procedures are presented in the supplemental Materials and Methods.

## RESULTS

*L-GILZ Isoform Is Expressed in Spermatogonia and in Primary Spermatocytes*—We have recently described a novel GILZ protein isoform, L-GILZ, that is involved in the regulation of cell growth and differentiation (28). L-GILZ comprises all characterized functional domains of GILZ including the N-terminal part encoded by an upstream alternative exon 1 (Fig. 1*A*). L-GILZ is transcribed from an independent promoter (28) and has distinct pattern of expression compared with GILZ, with highest expression observed in testis where L-GILZ is the only detectable isoform (Fig. 1, *B* and *C*). Testicular expression of L-GILZ is confined to the germ cell lineage as Sertoli and Leydig cells are completely devoid of L-GILZ (Fig. 1*D*). During the first wave of spermatogenesis, L-GILZ is expressed in spermatogonia and spermatocytes until the early prophase I (leptotene, zygotene), as indicated by morphological criteria (Fig. 1*D*). It is not detected in late meiotic (pachytene and diplotene spermatocytes) and postmeiotic cells (spermatids and spermatozoa) (Fig. 1*D*), suggesting that L-GILZ plays a role in early stages of spermatogenesis.

The SSCs are part of a subset of germ cells called undifferentiated spermatogonia (6, 8, 29). This subset includes Asingle spermatogonia, which are thought to be the SSCs, that either self-renew by mitotic division or divide into Apaired and Aaligned spermatogonia. Using PLZF expression as a marker of undifferentiated and early dividing spermatogonia (4) (Asingle, Apaired, and Aaligned), we detected L-GILZ in PLZF-positive cells as well as in more differentiated PLZF-negative spermatogonia (Fig. 1*E*). Therefore, the L-GILZ expression pattern suggests that L-GILZ could be involved in spermatogenesis by regulating undifferentiated spermatogonia function.

*Lack of L-GILZ Impairs Spermatogenesis*—We generated *gilz* KO mice by a standard LoxP-Cre approach (Fig. 2*A*). The *gilz* gene is located in the X chromosome and is composed of 6 exons (30). A targeting vector was constructed by placing one LoxP site upstream of the coding exon 6 that is the largest coding exon and is common to all of the *gilz* isoforms, and a second LoxP site linked to a SV40-neomycin (SV40-neo) selectable marker downstream of exon 6 (Fig. 2*A*). SV40-neo cassette was flanked by FRT sites to allow its subsequent deletion *in vivo* by Flp recombination. The floxed allele of the *gilz* gene was generated through homologous recombination in C57BL/6 mouse embryonic stem (ES) cells. Two positive ES clones were used to produce chimeras. Correct targeted clones were determined by Southern blot analysis (Fig. 2*B*). Two chimeras have transmitted targeted modification through the germ line ($gilz^{flox/y}$ males and $gilz^{flox/+}$ females). We first generated a total *gilz* KO mice by crossing "floxed" *gilz* mice with general Cre-Deletor mice (31) that express CMV-CRE transgene starting from oocytes and mediate Cre-mediated excision at early embryonic stages of development generating "general" KO of *gilz* mice (here called *gilz* KO mice). Cre-mediated deletion of floxed exon 6 is expected to result in premature termination of *gilz* protein translation and destabilization of the truncated transcript (Fig. 2, *C* and *D*). *Gilz* KO mice are born at Mendelian ratios with the expected sex distribution and appear overtly normal. However, we found a dramatic phenotype in *gilz* KO testis, with a 70–80% reduction in testis size and weight compared with the WT littermate controls (Fig. 3, *A* and *B*). Moreover, when three *gilz* KO males were each mated with two females, none of the females became pregnant in a 6-month time period, indicating that although *gilz* KO males are viable and healthy at birth and adulthood, they are sterile. The seminiferous tubules in *gilz* KO mice rapidly lost all germ lineage cells (Fig. 3, *C* and *D*, and supplemental Fig. S1, *A* and *B*). In fact, adult *gilz* KO testes contained seminiferous tubules totally devoid of germ cells, with only GATA-1-positive Sertoli cells (32) remaining (Fig. 3, *E* and *F*). Analysis of testis cell count after birth reveals that the number of PLZF-positive cells decrease over time and completely disappear in adult *gilz* KO testes, suggesting a progressive loss of all germ cells including SSC (Fig. 3, *G*–*I*). Of note, gene expression analysis of germ lineage markers (1, 2) confirmed the absence of Oct-4, Nanos2, DAZL, or Mvh transcripts in adult *gilz* KO testis, whereas SOX-9 and luteinizing hormone receptor, markers of Sertoli and Leydig cells, respectively (2), were present (supplemental Fig. S1*C*).

Histological analysis aimed to define when, during spermatogenesis, *gilz* KO cells are lost showed no obvious differences in WT and *gilz* KO testes at birth (supplemental Fig. S1, *A* and *B*). However, differential numbers of germ cells were observed starting from 7 dpp. The number of *gilz* KO germ cells/tubule was higher at 7 dpp and decreased significantly at 14 dpp when spermatocytes progress through the pachytene stage of meiosis (supplemental Fig. S1, *A* and *B*). During the first meiotic phase we observed *gilz* KO tubule atypical spermatocytes containing condensed or scattered chromatin, showing a strong increase in histone H2AX phosphorylation (γH2AX), which is normally associated with double-strand breaks and genomic instability (supplemental Fig. S1*D*). Massive apoptosis was demonstrated in 14-dpp KO testes by TUNEL assay (supplemental Fig. S2, *A* and *B*). Consequently, round spermatids of the postmeiotic phases of differentiation were never found in 21-dpp *gilz* KO

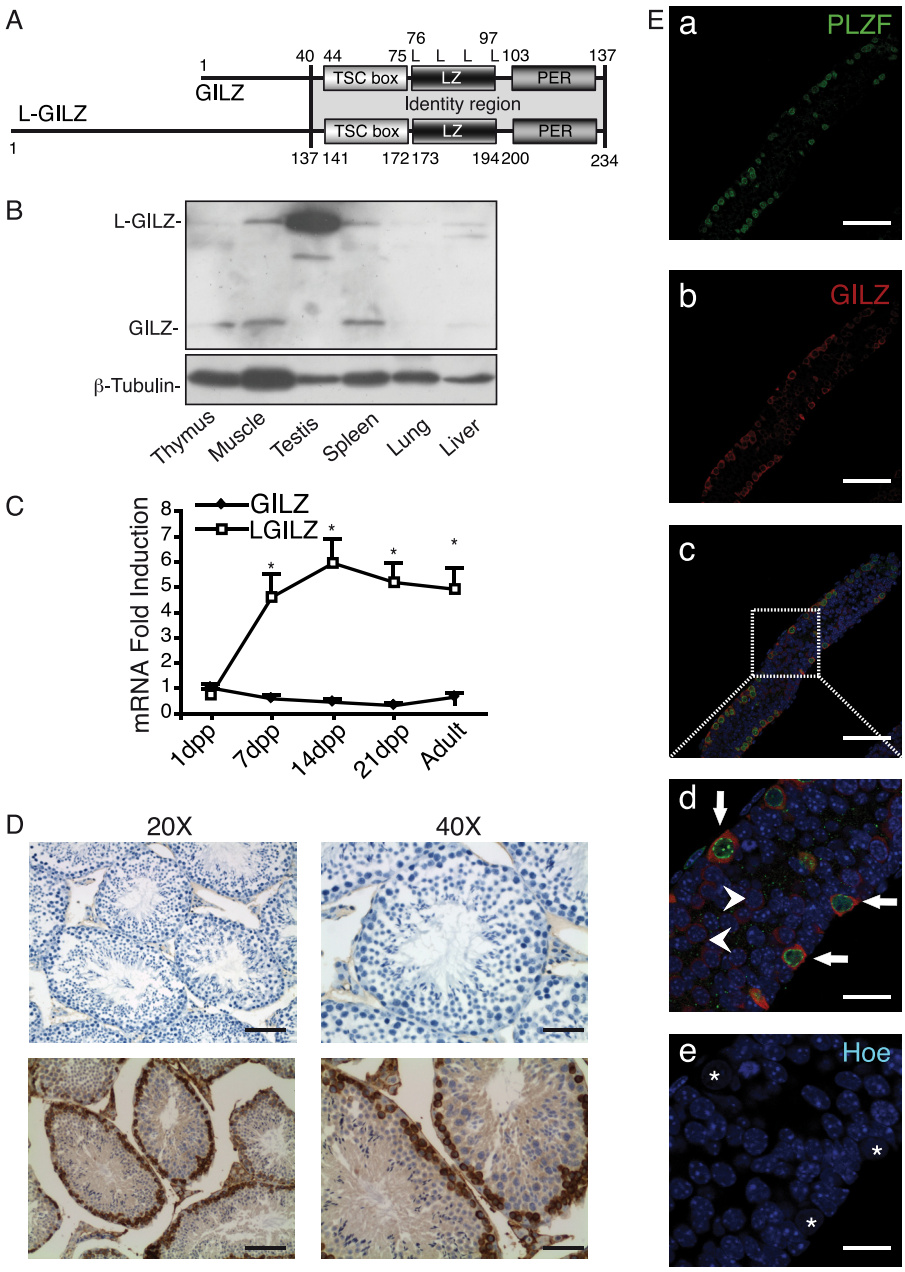


FIGURE 1. **L-GILZ is highly expressed in spermatogonia and primary spermatocytes.** *A*, graphical representation of conserved protein domains of *gilz* isoforms. The two proteins share an amino acid sequence that includes TGF $\beta$-stimulated clone box (*TSC box*), leucine zipper domain (*LZ*), and PER region (*PER*). *L*, leucine residues. *B*, L-GILZ protein expression in different murine tissues evaluated by Western blot analysis. $n = 3$ mice/group. *C*, GILZ and L-GILZ mRNA expression in testis at different ages evaluated by qPCR. GILZ expression in 1-dpp WT testis was arbitrarily considered as a unit. Results are shown as means $\pm$ S.E. (*error bars*); $n = 5$ mice/group. *, $p < 0,05$, two-tailed Student's *t* test. *D*, L-GILZ expression in adult testis. Immunohistochemical analyses show that L-GILZ expression in testis is restricted to germ cells. *Upper panels*, isotype control. *Lower panels*, L-GILZ staining. *Scale bars*, 100 $\mu$m (magnification, $\times$20); 50 $\mu$m ($\times$40). *E*, whole mount immunostaining in 9-dpp testes with anti-GILZ (*red*) and anti-PLZF (*green*) antibodies. *a–c*, low magnification; *scale bars*, 75 $\mu$m). *d* and *e*, high magnification image (*scale bars*, 20 $\mu$m) showing co-expression of L-GILZ and PLZF (*white arrows*) in spermatogonia with large nuclei and the absence of chromocenters (*white asterisks*) as evidenced by Hoechst 33342 staining (*Hoe*). *Arrowheads* indicate L-GILZ expression in PLZF-negative spermatogonia.

testes (supplemental Fig. S1, *A* and *B*). To note, no increase in cell death was observed at the premeiotic stage of differentiation before 10 dpp, as indicated by TUNEL assay and gene expression analysis of apoptosis-related genes (supplemental Fig. S2, *C* and *D*). These results demonstrate that lack of L-GILZ leads to a complete depletion of the germ cell lineage, including SSCs, resembling the phenotype occurring in the human Sertoli cell-only syndrome (33). Thus, L-GILZ is essential for spermatogenesis.

*Spermatogenesis Failure in Gilz KO Mice Is Intrinsic to Germ Cells*—Pituitary gland-derived gonadotropins luteinic hormone (LH) and follicle-stimulating hormone (FSH) control the physiological activity of Sertoli and Leydig cells, both essential for regulation of germ cell function. Spermatogenesis is also controlled by steroid hormones produced by Leydig cells (34). To rule out the possibility that defects in cells other than of the germ lineage contribute to cell depletion in *gilz* KO animals, we first analyzed spermatogenesis-related hormone levels (34). LH

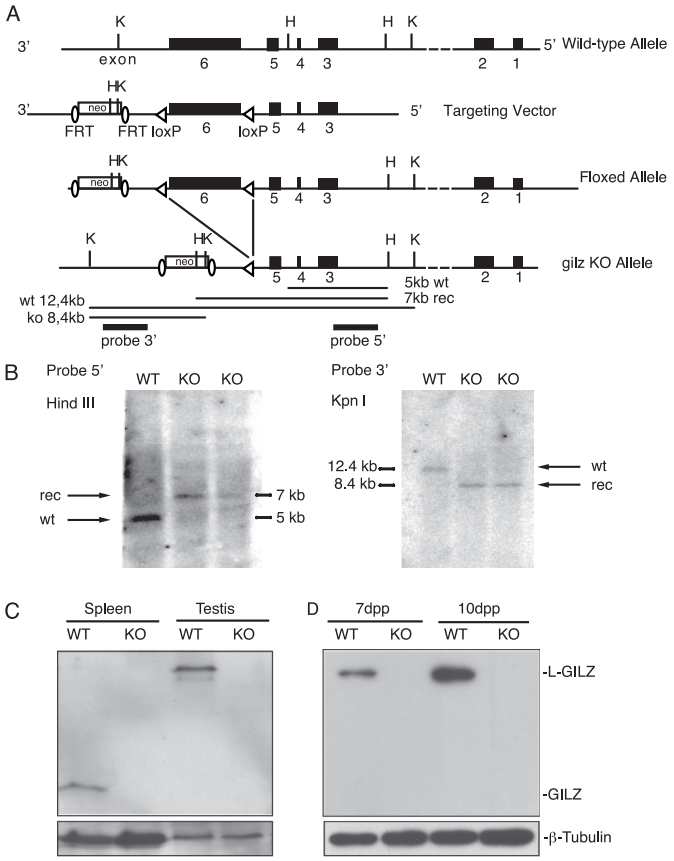


FIGURE 2. **Targeted disruption of murine *gilz* gene.** *A*, schematic representations of WT allele, targeting vector, floxed and recombinant locus of *gilz* gene. *K*, KpnI; *H*, HindIII. *B*, genotype analysis of WT and *gilz* KO mice. Genomic DNA was isolated from mice tails, and genotypes were determined by Southern blot analysis with 5′ and 3′ probes represented with *black boxes* below the *gilz* KO allele in *C*. The 5′ probe hybridized to 5-kb (WT) and 7-kb (targeted) HindIII fragments. The 3′ probe hybridized to 12.4-kb (WT) and 8.4-kb (targeted) KpnI fragments. *C*, Western blot analysis of spleen and testis of WT or *gilz* KO adult mice. Figure is representative of three different experiments. *D*, Western blot analysis of 7-dpp and 10-dpp WT or *gilz* KO testis. Figure is representative of three different experiments.

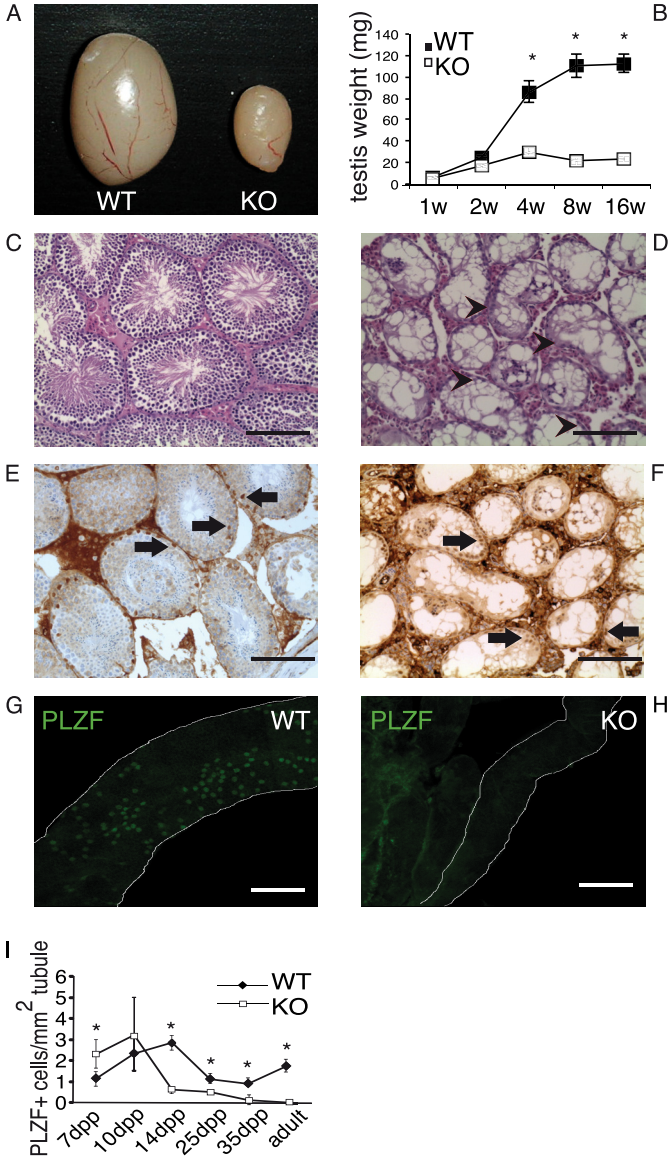


FIGURE 3. **GILZ is necessary for normal spermatogenesis.** *A*, testis from 12-week-old WT and *gilz* KO mice. *B*, average ratio of body/testis body weight at different ages as indicated in the figure. Results are shown as means ± S.E. (*error bars*); $n = 10$ mice/group. *, $p < 0.05$, two-tailed Student's *t* test. *C* and *D*, histology of WT and *gilz* KO adult testis. *Gilz* KO tubules contain only Sertoli cells (*arrowheads*). *Scale bars*, 100 μm. *E* and *F*, immunohistochemistry for GATA-1 staining. *Gilz* KO adult testis contains only GATA-1-positive cells (*F*, *black arrows*). Scale bars, 100 μm. *G* and *H*, loss of PLZF-positive cells in *gilz* KO adult testis. *Scale bars*, 100 μm. *I*, quantitative analysis of PLZF-expressing cells. 10 different sections of testes of each genotype were randomly selected. The average numbers of PLZF-positive cells/area of each mouse were calculated at each time point; results are shown as means ± S.E.; $n = 5$ mice per group. *, $p < 0.05$, two-tailed Student's *t* test.

and FSH levels in the pituitary gland as well as serum testosterone were similar in WT and *gilz* KO mice (supplemental Fig. S3, *A* and *C*). No differences were observed in estrogen receptor, androgen receptor, FSH receptor, and LH receptor expression (supplemental Fig. S3*B*). To prove that the defect in spermatogenesis was not due to a stem cell niche dysfunction or to abnormalities in the hypothalamic-pituitary-gonadal axis, we crossed $gilz^{flox/y}$ males with mice carrying the Mvh-Cre transgene to generate germ cell-specific *gilz* KO mice (*gilz* cKO). As in the *gilz* KO mice, the tubules of germ cell-specific *gilz* cKO adult testes were devoid of germ cells (supplemental Fig. S4*A*) and lacked the expression of germ stem cell markers (supplemental Fig. S4*B*). The ultimate proof that defective spermatogenesis in *gilz* KO mice is intrinsic to germ cells was given by transplantation of WT germ cells into *gilz* KO testis, in which we were able to restore normal spermatogenesis in recipient mice (supplemental Fig. S4, *C–F*), indicating that recipient *gilz* KO testis was able to support normal spermatogenesis by functional WT germ cells. These results demonstrate that failure of spermatogenesis is caused by the absence of L-GILZ in germ cells.

*Increased Proliferation and Differentiation in Gilz KO Undifferentiated Spermatogonia*—To elucidate the molecular defects leading to spermatogenesis failure in *gilz* KO mice we performed gene expression profiling of WT and *gilz* KO testes at 7 dpp, when the phenotypic differences become evident. Microarray and qPCR analysis revealed deregulation of expression of relatively few genes (Fig. 4*A* and supplemental Table S1). Nevertheless, important differences between *gilz* KO and WT testes were revealed by Gene Set Enrichment Analysis such as the deregulation of cell cycle-related gene sets, suggesting that

**A**

| Fold change KO vs WT | | |
|---|---|---|
| Gene | Array | qPCR |
| Gfra1 | 0,68 | 0,53 |
| Ret | 0,59 | 0,49 |
| Gdnf | 0,899 | 1,00 |
| Neurog3 | 0,645 | 0,21 |
| Oct4 | 0,955 | 0,42 |
| Nanos2 | 0,874 | 0,30 |
| Mvh | 0,965 | 0,60 |
| Sohlh2 | 1,552 | 1,41 |
| Sycp3 | 1,466 | 1,62 |
| Sycp1 | 1,551 | 2,04 |
| Sycp2 | 1,414 | 1,24 |
| Xmr | 1,814 | 1,98 |
| Megea3 | 1,966 | 2,80 |
| Megea2 | 1,828 | 1,99 |
| Megea5 | 1,912 | 3,35 |
| Megea1 | 1,959 | 2,90 |
| Megea6 | 2,146 | 2,89 |
| Actb | 0,983 | 1,04 |

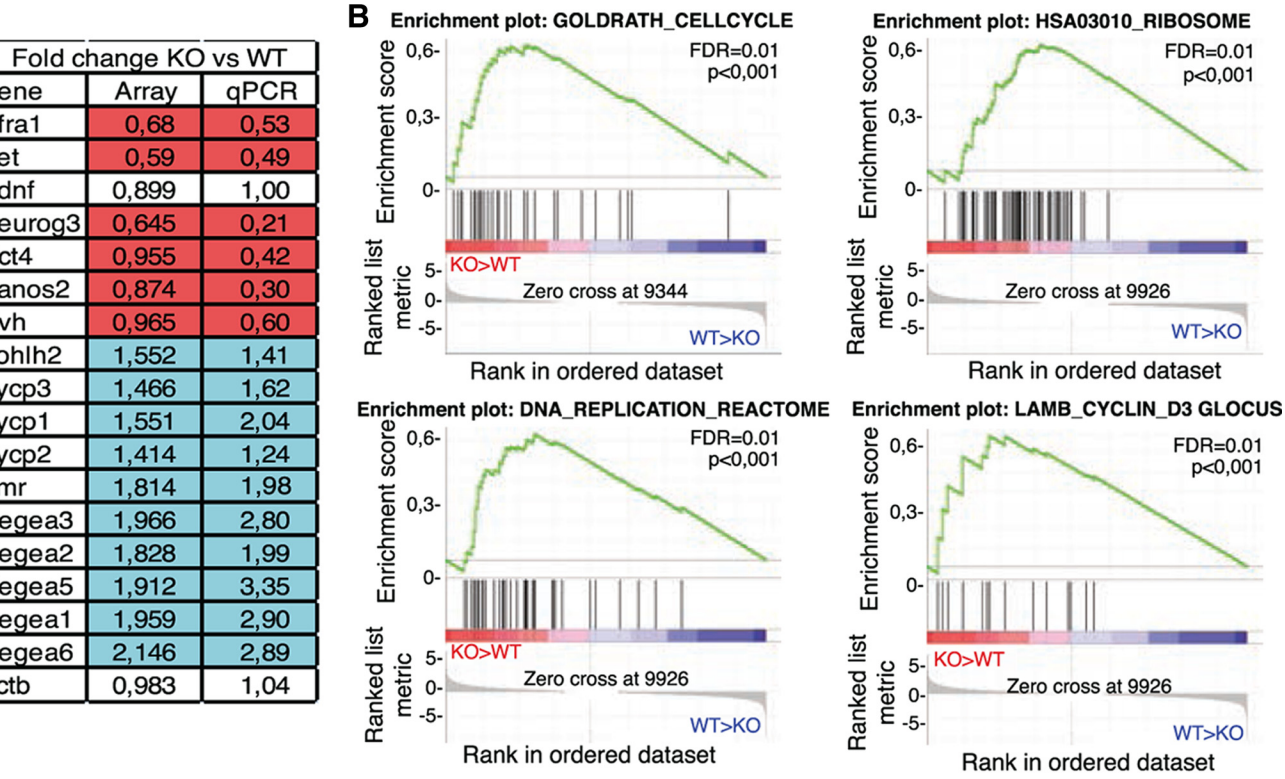


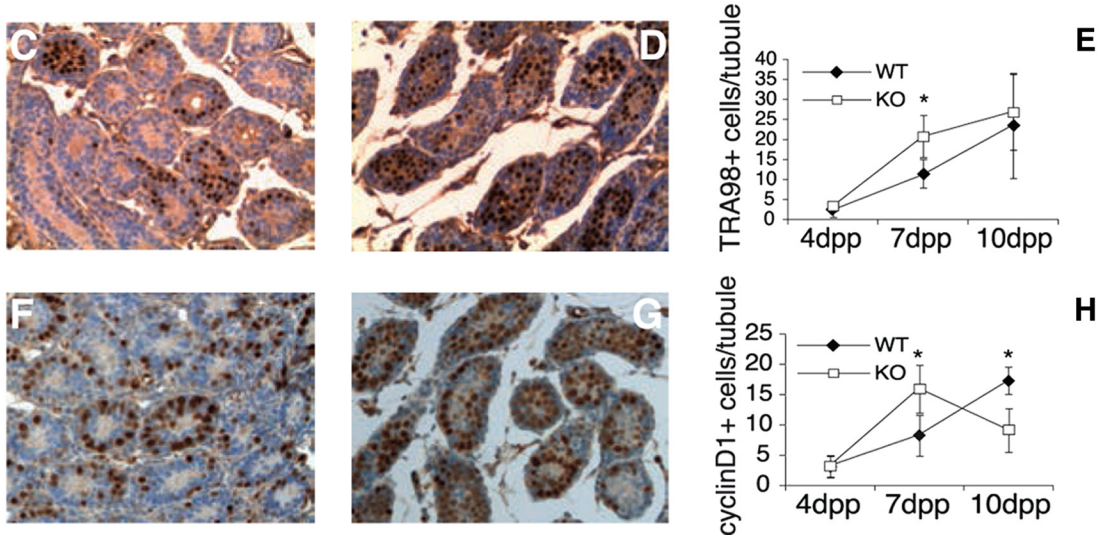


FIGURE 4. **Increased proliferation and differentiation in spermatogonia of *gilz* KO neonatal mice.** *A*, microarray analysis of gene expression in testis from 7-dpp WT and *gilz* KO mice. Results are visualized in the *table* as relative -fold changes between *gilz* KO *versus* WT. Expression of selected genes identified in the microarray analysis was validated by qPCR (*right column*) using as template an aliquot of the same RNA used for microarray (up-regulated genes in *blue*, and down-regulated genes in *red*). 18 samples were pooled in six groups, each made of three biological replicates. The two experimental groups were: 7-dpp WT and 7-dpp KO. Global variation over genotype results in 36 genes selected for *p* value and -fold change. The analysis indicates that variation in these contrasts is low, and WT and *gilz* KO results yield 59 differentially expressed genes (supplemental Table S1). *B*, GSEA analysis identified enrichment of proliferation-related gene sets in *gilz* KO testis. Enrichment profile describes positively correlated KO gene set represented on the *left* part of each graph (*red bar*) and negatively correlated WT gene sets on the *right* part (*blue bar*). The enrichment score curves were obtained from GSEA software. *C–H*, immunohistochemical analyses of TRA98 and cyclin D1 expression in sections of postnatal testis at different stages of development. Numbers of both TRA98$^+$ (*C–E*) and cyclin D1$^+$ (*F–H*) cells are significantly higher in 7-dpp *gilz* KO testis compared with controls. *Scale bars*, 100 $\mu$m. The average numbers of TRA98$^+$ or Cyclin D1$^+$ cells/area of each section were calculated at each time point and are represented in the *graphic charts*; results are shown as means ± S.E. (*error bars*); $n = 5$ mice/group. *, $p < 0.05$, two-tailed Student's *t* test.

*gilz* KO spermatogonia proliferate faster (Fig. 4*B*). Consistently, 7-dpp and 10-dpp testes of *gilz* KO mice had significantly more TRA98-positive germ cells (7) (Fig. 4, *C–E*), and tubules contained more cells positive for cyclin D1 (Fig. 4, *F–H*), a marker of mitotically active spermatogonia (35). In addition, we also observed down-regulation of glial cell line-derived neurotrophic factor receptor (GFR)$\alpha$-1/Ret, components of glial cell-derived neurotrophic factor receptor shown to be essential for SSC self-renewal (5, 36) (Fig. 4*A*). Notably, expression of factors regulating spermatogonia differentiation such as

Sohlh-2, scp1, scp2, scp3, and xmr (37, 38) (Fig. 4*A*) was increased in *gilz* KO testis. Moreover, magea-1, -2, -3, -5, and -6 transcripts, which are specifically expressed at a later stage of differentiation (39), were expressed in *gilz* KO testis (Fig. 4*A*). Altogether, these data indicate that L-GILZ absence leads to enhanced proliferation and differentiation of undifferentiated spermatogonia thus suggesting that L-GILZ regulates spermatogonial function.

To address the role of L-GILZ in control of spermatogonia proliferation, we performed BrdU incorporation assay in 7-dpp spermatogonia. The degree of BrdU incorporation was evaluated in spermatogonia expressing α6-int, a marker of germ cell lineage, positive or negative for expression of c-Kit, a marker of differentiating spermatogonia (40). Undifferentiated α6-int-positive (α6-int$^+$) and c-Kit negative (c-Kit$^-$) spermatogonia showed a 2-fold increase in BrdU incorporation in *gilz* KO compared with WT cells (Fig. 5, *A–C*), indicating that *gilz* KO undifferentiated spermatogonia are cycling faster. At the same time, we observed an accumulation of differentiating spermatogonia as the frequency of α6-int$^+$/c-Kit$^+$ subset increased significantly in *gilz* KO testis (Fig. 5*D*). These data indicate that α6-int$^+$/c-Kit$^-$ undifferentiated subset had a higher proliferation rate.

*GILZ Regulates Ras Pathway in Undifferentiated Spermatogonia*—It is known that the Ras signaling pathway is a key regulator of spermatogonia proliferation (41–43). Moreover, it has been shown previously that GILZ binds Ras and inhibits Ras-dependent cell proliferation (26). Here, we found that the L-GILZ, similar to GILZ, is able to bind Ras in transient transfection co-immunoprecipitation experiments (Fig. 6*A*). To evaluate whether the L-GILZ absence leads to the activation of Ras intracellular signaling cascade in undifferentiated spermatogonia, we compared the levels of the activated form of ERK and Akt in α6-int$^+$/c-Kit$^-$ WT and *gilz* KO spermatogonia, by measuring ERK and Akt phosphorylation. We found increased levels of ERK and Akt phosphorylation suggesting that L-GILZ regulates the Ras signaling in undifferentiated spermatogonia (Fig. 6, *B–D*). Pharmacologic inhibition of Akt was able to revert increased BrdU uptake by α6-int$^+$/c-Kit$^-$ *gilz* KO spermatogonia, further suggesting that Akt activity downstream of Ras contributes to a hyperproliferative phenotype of *gilz* KO spermatogonia (Fig. 6*E*). Consistent with increased ERK and Akt phosphorylation and cell proliferation, we also found an increased level of cyclin D1 expression in *gilz* KO α6-int$^+$/c-Kit$^-$ spermatogonia (Fig. 6, *F* and *G*). Together, our results suggest that L-GILZ controls Ras signaling and inhibits undifferentiated spermatogonia proliferation.

## DISCUSSION

We here show that L-GILZ, a longer isoform of previously described GILZ, is highly expressed in germ lineage and is required for its maintenance. In particular, deletion of *gilz* gene in the whole mouse as well as specifically in germ cell lineage resulted in a drastic phenotype characterized by germ cell loss associated with altered undifferentiated spermatogonia proliferation, aberrant differentiation, and massive apoptosis during the first meiotic stage.

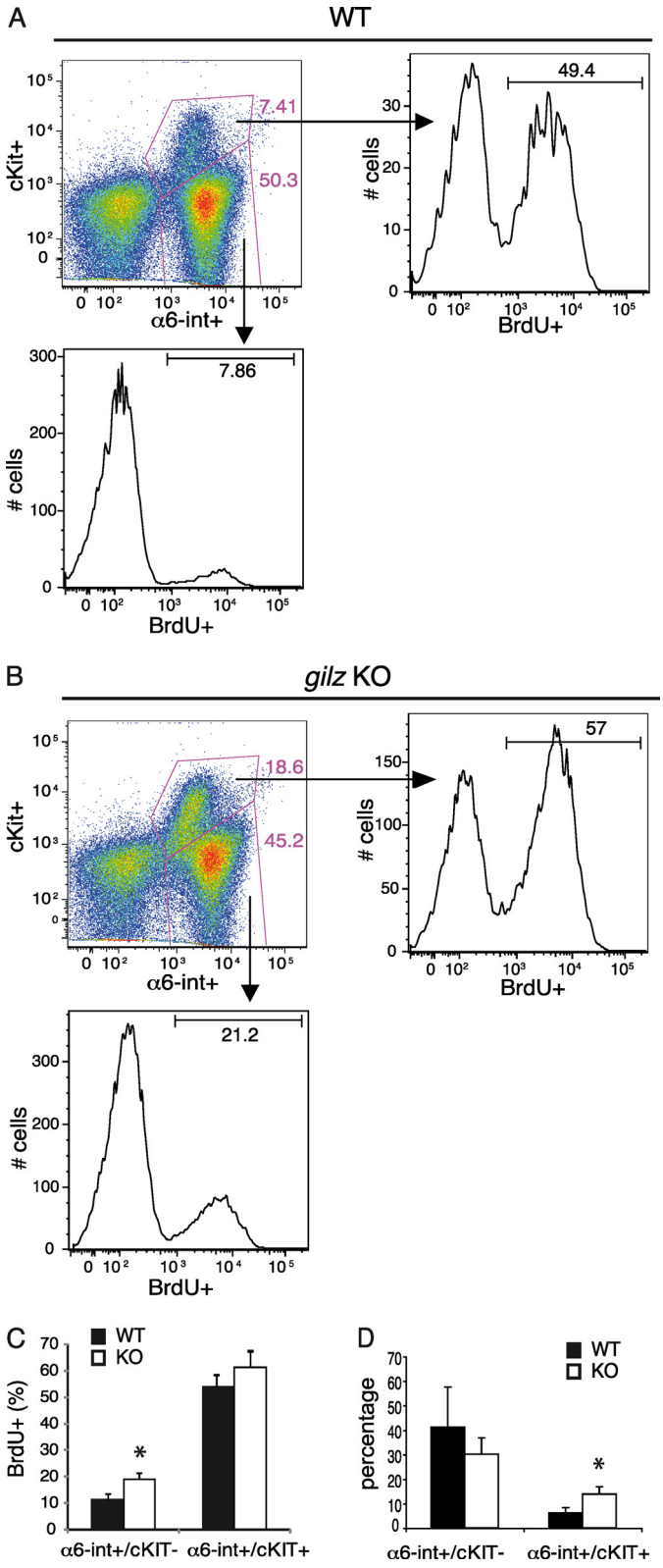


FIGURE 5. **L-GILZ regulates spermatogonia proliferation and differentiation.** *A* and *B*, α6-int and c-Kit expression in WT and *gilz* KO spermatogonia. Frequency of spermatogonia subsets α6-int$^+$/c-Kit$^+$ and α6-int$^+$/c-Kit$^-$ are indicated in the *dot plots* and in *graph* in *D* (mean ± S.E., $n = 6$). *Histograms* represents levels of BrdU incorporation in the indicated plots. *A–C*, proliferation of different spermatogonia populations assessed by *in vitro* BrdU incorporation. The *bar graphs* in *C* and D represent results from three independent experiments means ± S.E. (*error bars*); $n = 6$ mice per group. *, $p < 0.05$, two-tailed Student's *t* test.

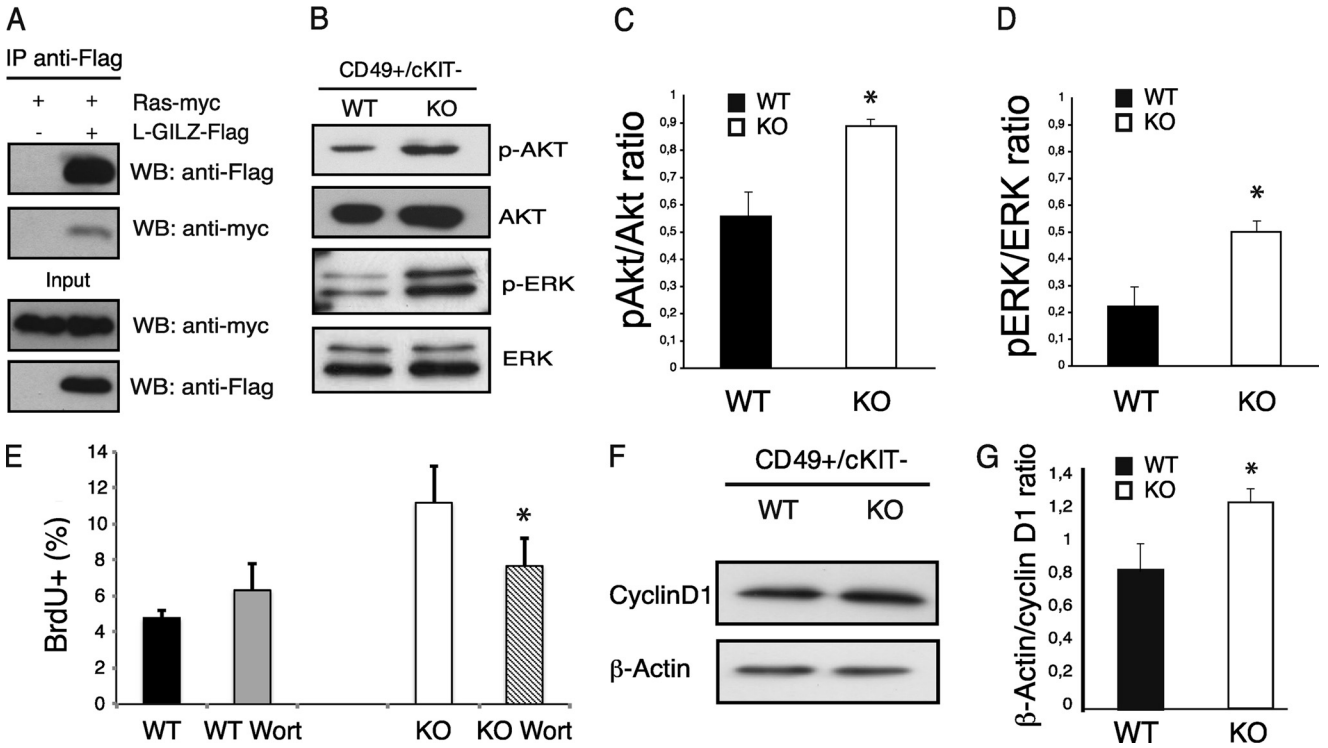


FIGURE 6. **L-GILZ binds Ras and regulates undifferentiated spermatogonia proliferation in Ras-dependent manner.** *A*, L-GILZ interacts with Ras. HEK293 cells were co-transfected with L-GILZ-FLAG and Ras-Myc expression vectors (*right lane*) or Ras-Myc alone (*left lane*). Immunoprecipitation (*IP*) was carried out with anti-FLAG M2 microbeads, and co-immunoprecipitation was revealed with anti-FLAG and anti-Myc antibodies. *WB*, Western blotting. *B–D*, phosphorylation of Akt (pAkt) and phospho-ERK (pERK) is increased in *gilz* KO $\alpha$6-int$^+$/c-Kit$^-$ spermatogonia 7 dpp as assessed by Western blot analysis. *Bars* in *C* and *D* represent densitometric analysis. Values were calculated based on the analysis of three separate blots ± S.E. (*error bars*). *, $p < 0{,}05$, two-tailed Student's *t* test. *E*, *in vitro* wortmannin treatment inhibits the hyperactivity of Akt pathway in $\alpha$6-int$^+$/c-Kit$^-$ *gilz* KO spermatogonia. *Graph bars* show mean results from three independent experiments ± S.E. *, $p < 0.05$, two-tailed Student's *t* test. *F*, expression of cyclin D1 is increased in *gilz* KO $\alpha$6-int$^+$/c-Kit$^-$ spermatogonia 7 dpp as assessed by Western blot analysis. *G*, densitometric analysis was calculated from three separate blots. Values are represented as mean of $\beta$-actin/cyclin D1 ratio ± S.E. *, $p < 0.05$, two-tailed Student's *t* test.

Previous studies showed that the shorter isoform GILZ can inhibit T cell activation/proliferation (22, 24, 26, 44–46). GILZ has also been shown to control proliferation and differentiation in other cell types including adipocytes, osteoblasts, and myoblasts (28, 47, 48). Conservation of most of the GILZ functional domains in L-GILZ isoform suggests that L-GILZ can act as suppressor of cell growth and differentiation.

Here, we demonstrate that L-GILZ, but not GILZ, is highly expressed in undifferentiated spermatogonia and in primary spermatocytes. Lack of L-GILZ results in complete loss of the whole germ cell lineage within few weeks after birth. No germ cells beyond pachytene spermatocytes were observed in *gilz* KO testis due to massive apoptosis during meiotic phase. No increase in apoptosis was found in *gilz* KO testis before meiosis entry, indicating that cells lacking L-GILZ die when they reach meiosis differentiation stage. Nevertheless, we do not observe accumulation of premeiotic spermatogonia in *gilz* KO testis. On the contrary, *gilz* KO mice have empty tubules, containing only Sertoli cells. L-GILZ is expressed not only in primary spermatocytes but also in spermatogonia, including PLZF-positive undifferentiated spermatogonia. The PLZF-positive cells gradually decrease over time and completely disappear in adult *gilz* KO testes, suggesting that L-GILZ plays also a role in undifferentiated spermatogonia, including SSCs.

We show that L-GILZ acts as an inhibitor of undifferentiated spermatogonia proliferation. In fact, lack of L-GILZ resulted in enhanced cycling of the less differentiated $\alpha$6-int$^+$/c-Kit$^-$ spermatogonia, with a concomitant increase frequency in $\alpha$6-int$^+$/c-Kit$^+$ differentiating spermatogonia.

It is known, on the basis of results obtained in many experimental models, that Ras signaling is important in controlling cell proliferation and differentiation (9, 12–15). Downstream effectors of Ras MAPK/ERK and PI3K/Akt signaling pathways have been shown to play an important role in controlling cell survival, proliferation, and differentiation in many experimental models including spermatogenesis (36, 42, 43, 49). GILZ-Ras interaction has been already characterized in other cell types, and it has been shown that GILZ is able to inhibit Ras signaling and cell proliferation (26). Here, we show that L-GILZ binds Ras, and *gilz* KO spermatogonia have enhanced Ras signaling. Moreover, *gilz* KO spermatogonia have an increased level of ERK and Akt phosphorylation, augmented cyclin D1 expression, and increased proliferation. These results are in line with many studies indicating an important role of Ras signaling in undifferentiated spermatogonia proliferation and differentiation (36, 42, 43, 50–52). Here, we show that a novel link L-GILZ-Ras emerges as a critical axis in the regulation of undifferentiated spermatogonia proliferation, differentiation, and survival.

In conclusion, this study demonstrates that lack of L-GILZ causes eradication of the germ cell lineage and male sterility with a phenotype similar to pathological features of Sertoli cell-

only syndrome (33). This phenotype is a combination of at least three steps: (i) acceleration of proliferation of undifferentiated spermatogonia associated with hyperactivated Ras signaling; (ii) aberrant spermatogonial differentiation; and (iii) massive apoptosis during meiotic phase. We cannot exclude that these events are linked, but more studies are needed to dissect further the role of L-GILZ in spermatogenesis. This discovery is a clear advance in our knowledge of the mechanisms underlying spermatogenesis and indicate L-GILZ as a possible target for novel therapies to intervene in male sterility.

*Acknowledgments—We thank Dr. Riccardo Dalla Favera for critical reading of the manuscript and Dr. Claus Nerlov for expert assistance and critical input in the early phases of this study.*

## REFERENCES


1. Wong, M. D., Jin, Z., and Xie, T. (2005) Molecular mechanisms of germline stem cell regulation. *Annu. Rev. Genet.* **39,** 173–195
2. Matzuk, M. M., and Lamb, D. J. (2008) The biology of infertility: research advances and clinical challenges. *Nat. Med.* **14,** 1197–1213
3. Buaas, F. W., Kirsh, A. L., Sharma, M., McLean, D. J., Morris, J. L., Griswold, M. D., de Rooij, D. G., and Braun, R. E. (2004) Plzf is required in adult male germ cells for stem cell self-renewal. *Nat. Genet.* **36,** 647–652
4. Costoya, J. A., Hobbs, R. M., Barna, M., Cattoretti, G., Manova, K., Sukhwani, M., Orwig, K. E., Wolgemuth, D. J., and Pandolfi, P. P. (2004) Essential role of Plzf in maintenance of spermatogonial stem cells. *Nat. Genet.* **36,** 653–659
5. Meng, X., Lindahl, M., Hyvönen, M. E., Parvinen, M., de Rooij, D. G., Hess, M. W., Raatikainen-Ahokas, A., Sainio, K., Rauvala, H., Lakso, M., Pichel, J. G., Westphal, H., Saarma, M., and Sariola, H. (2000) Regulation of cell fate decision of undifferentiated spermatogonia by GDNF. *Science* **287,** 1489–1493
6. Oatley, J. M., and Brinster, R. L. (2008) Regulation of spermatogonial stem cell self-renewal in mammals. *Annu. Rev. Cell Dev. Biol.* **24,** 263–286
7. Sada, A., Suzuki, A., Suzuki, H., and Saga, Y. (2009) The RNA-binding protein NANOS2 is required to maintain murine spermatogonial stem cells. *Science* **325,** 1394–1398
8. Nakagawa, T., Sharma, M., Nabeshima, Y., Braun, R. E., and Yoshida, S. (2010) Functional hierarchy and reversibility within the murine spermatogenic stem cell compartment. *Science* **328,** 62–67
9. Katz, M. E., and McCormick, F. (1997) Signal transduction from multiple Ras effectors. *Curr. Opin. Genet. Dev.* **7,** 75–79
10. Vojtek, A. B., and Der, C. J. (1998) Increasing complexity of the Ras signaling pathway. *J. Biol. Chem.* **273,** 19925–19928
11. Tartaglia, M., and Gelb, B. D. (2010) Disorders of dysregulated signal traffic through the RAS-MAPK pathway: phenotypic spectrum and molecular mechanisms. *Ann. N.Y. Acad. Sci.* **1214,** 99–121
12. Gille, H., and Downward, J. (1999) Multiple ras effector pathways contribute to G(1) cell cycle progression. *J. Biol. Chem.* **274,** 22033–22040
13. Lavoie, J. N., L'Allemain, G., Brunet, A., Müller, R., and Pouysségur, J. (1996) Cyclin D1 expression is regulated positively by the p42/p44MAPK and negatively by the p38/HOGMAPK pathway. *J. Biol. Chem.* **271,** 20608–20616
14. Mirza, A. M., Gysin, S., Malek, N., Nakayama, K., Roberts, J. M., and McMahon, M. (2004) Cooperative regulation of the cell division cycle by the protein kinases RAF and AKT. *Mol. Cell. Biol.* **24,** 10868–10881
15. Muise-Helmericks, R. C., Grimes, H. L., Bellacosa, A., Malstrom, S. E., Tsichlis, P. N., and Rosen, N. (1998) Cyclin D expression is controlled post-transcriptionally via a phosphatidylinositol 3-kinase/Akt-dependent pathway. *J. Biol. Chem.* **273,** 29864–29872
16. Kolch, W. (2005) Coordinating ERK/MAPK signalling through scaffolds and inhibitors. *Nat. Rev. Mol. Cell Biol.* **6,** 827–837
17. Morrison, D. K., and Davis, R. J. (2003) Regulation of MAP kinase signaling modules by scaffold proteins in mammals. *Annu. Rev. Cell Dev. Biol.* **19,** 91–118
18. Irie, K., Gotoh, Y., Yashar, B. M., Errede, B., Nishida, E., and Matsumoto, K. (1994) Stimulatory effects of yeast and mammalian 14-3-3 proteins on the Raf protein kinase. *Science* **265,** 1716–1719
19. Li, W., Han, M., and Guan, K. L. (2000) The leucine-rich repeat protein SUR-8 enhances MAP kinase activation and forms a complex with Ras and Raf. *Genes Dev.* **14,** 895–900
20. Matheny, S. A., Chen, C., Kortum, R. L., Razidlo, G. L., Lewis, R. E., and White, M. A. (2004) Ras regulates assembly of mitogenic signalling complexes through the effector protein IMP. *Nature* **427,** 256–260
21. Wang, H. G., Takayama, S., Rapp, U. R., and Reed, J. C. (1996) Bcl-2 interacting protein, BAG-1, binds to and activates the kinase Raf-1. *Proc. Natl. Acad. Sci. U.S.A.* **93,** 7063–7068
22. Ayroldi, E., Migliorati, G., Bruscoli, S., Marchetti, C., Zollo, O., Cannarile, L., D'Adamio, F., and Riccardi, C. (2001) Modulation of T-cell activation by the glucocorticoid-induced leucine zipper factor via inhibition of nuclear factor κB. *Blood* **98,** 743–753
23. Ayroldi, E., and Riccardi, C. (2009) Glucocorticoid-induced leucine zipper (GILZ): a new important mediator of glucocorticoid action. *FASEB J.* **23,** 3649–3658
24. D'Adamio, F., Zollo, O., Moraca, R., Ayroldi, E., Bruscoli, S., Bartoli, A., Cannarile, L., Migliorati, G., and Riccardi, C. (1997) A new dexamethasone-induced gene of the leucine zipper family protects T lymphocytes from TCR/CD3-activated cell death. *Immunity* **7,** 803–812
25. Riccardi, C., Bruscoli, S., Ayroldi, E., Agostini, M., and Migliorati, G. (2001) GILZ, a glucocorticoid hormone induced gene, modulates T lymphocytes activation and death through interaction with NF-κB. *Adv. Exp. Med. Biol.* **495,** 31–39
26. Ayroldi, E., Zollo, O., Bastianelli, A., Marchetti, C., Agostini, M., Di Virgilio, R., and Riccardi, C. (2007) GILZ mediates the antiproliferative activity of glucocorticoids by negative regulation of Ras signaling. *J. Clin. Invest.* **117,** 1605–1615
27. Ayroldi, E., Zollo, O., Macchiarulo, A., Di Marco, B., Marchetti, C., and Riccardi, C. (2002) Glucocorticoid-induced leucine zipper inhibits the Raf-extracellular signal-regulated kinase pathway by binding to Raf-1. *Mol. Cell. Biol.* **22,** 7929–7941
28. Bruscoli, S., Donato, V., Velardi, E., Di Sante, M., Migliorati, G., Donato, R., and Riccardi, C. (2010) Glucocorticoid-induced leucine zipper (GILZ) and long GILZ inhibit myogenic differentiation and mediate anti-myogenic effects of glucocorticoids. *J. Biol. Chem.* **285,** 10385–10396
29. de Rooij, D. G. (2009) The spermatogonial stem cell niche. *Microsc. Res. Tech.* **72,** 580–585
30. Cannarile, L., Zollo, O., D'Adamio, F., Ayroldi, E., Marchetti, C., Tabilio, A., Bruscoli, S., and Riccardi, C. (2001) Cloning, chromosomal assignment and tissue distribution of human GILZ, a glucocorticoid hormone-induced gene. *Cell Death Differ.* **8,** 201–203
31. Su, H., Mills, A. A., Wang, X., and Bradley, A. (2002) A targeted X-linked CMV-Cre line. *Genesis* **32,** 187–188
32. Yomogida, K., Ohtani, H., Harigae, H., Ito, E., Nishimune, Y., Engel, J. D., and Yamamoto, M. (1994) Developmental stage- and spermatogenic cycle-specific expression of transcription factor GATA-1 in mouse Sertoli cells. *Development* **120,** 1759–1766
33. Chaganti, R. S., Jhanwar, S. C., Ehrenbard, L. T., Kourides, I. A., and Williams, J. J. (1980) Genetically determined asynapsis, spermatogenic degeneration, and infertility in men. *Am. J. Hum. Genet.* **32,** 833–848
34. Sharpe, R. M., McKinnell, C., Kivlin, C., and Fisher, J. S. (2003) Proliferation and functional maturation of Sertoli cells, and their relevance to disorders of testis function in adulthood. *Reproduction* **125,** 769–784
35. Beumer, T. L., Roepers-Gajadien, H. L., Gademan, I. S., Kal, H. B., and de Rooij, D. G. (2000) Involvement of the D-type cyclins in germ cell proliferation and differentiation in the mouse. *Biol. Reprod.* **63,** 1893–1898
36. Oatley, J. M., Avarbock, M. R., and Brinster, R. L. (2007) Glial cell line-derived neurotrophic factor regulation of genes essential for self-renewal of mouse spermatogonial stem cells is dependent on Src family kinase signaling. *J. Biol. Chem.* **282,** 25842–25851
37. Calenda, A., Allenet, B., Escalier, D., Bach, J. F., and Garchon, H. J. (1994) The meiosis-specific *Xmr* gene product is homologous to the lymphocyte Xlr protein and is a component of the XY body. *EMBO J.* **13,** 100–109

38. Wang, P. J., and Pan, J. (2007) The role of spermatogonially expressed germ cell-specific genes in mammalian meiosis. *Chromosome Res.* **15,** 623–632
39. Clotman, F., De Backer, O., De Plaen, E., Boon, T., and Picard, J. (2000) Cell- and stage-specific expression of mage genes during mouse spermatogenesis. *Mamm. Genome* **11,** 696–699
40. Blume-Jensen, P., Jiang, G., Hyman, R., Lee, K. F., O'Gorman, S., and Hunter, T. (2000) Kit/stem cell factor receptor-induced activation of phosphatidylinositol 3′-kinase is essential for male fertility. *Nat. Genet.* **24,** 157–162
41. Almog, T., and Naor, Z. (2008) Mitogen-activated protein kinases (MAPKs) as regulators of spermatogenesis and spermatozoa functions. *Mol. Cell. Endocrinol.* **282,** 39–44
42. He, Z., Jiang, J., Kokkinaki, M., Golestaneh, N., Hofmann, M. C., and Dym, M. (2008) Gdnf upregulates c-Fos transcription via the Ras/Erk1/2 pathway to promote mouse spermatogonial stem cell proliferation. *Stem Cells* **26,** 266–278
43. Lee, J., Kanatsu-Shinohara, M., Morimoto, H., Kazuki, Y., Takashima, S., Oshimura, M., Toyokuni, S., and Shinohara, T. (2009) Genetic reconstruction of mouse spermatogonial stem cell self-renewal *in vitro* by Ras-cyclin D2 activation. *Cell Stem Cell* **5,** 76–86
44. Cannarile, L., Cuzzocrea, S., Santucci, L., Agostini, M., Mazzon, E., Esposito, E., Muià, C., Coppo, M., Di Paola, R., and Riccardi, C. (2009) Glucocorticoid-induced leucine zipper is protective in Th1-mediated models of colitis. *Gastroenterology* **136,** 530–541
45. Cannarile, L., Fallarino, F., Agostini, M., Cuzzocrea, S., Mazzon, E., Vacca, C., Genovese, T., Migliorati, G., Ayroldi, E., and Riccardi, C. (2006) Increased GILZ expression in transgenic mice up-regulates Th-2 lymphokines. *Blood* **107,** 1039–1047
46. Di Marco, B., Massetti, M., Bruscoli, S., Macchiarulo, A., Di Virgilio, R., Velardi, E., Donato, V., Migliorati, G., and Riccardi, C. (2007) Glucocorticoid-induced leucine zipper (GILZ)/NF-κB interaction: role of GILZ homo-dimerization and C-terminal domain. *Nucleic Acids Res.* **35,** 517–528
47. Shi, X., Shi, W., Li, Q., Song, B., Wan, M., Bai, S., and Cao, X. (2003) A glucocorticoid-induced leucine-zipper protein, GILZ, inhibits adipogenesis of mesenchymal cells. *EMBO Rep.* **4,** 374–380
48. Zhang, W., Yang, N., and Shi, X. M. (2008) Regulation of mesenchymal stem cell osteogenic differentiation by glucocorticoid-induced leucine zipper (GILZ). *J. Biol. Chem.* **283,** 4723–4729
49. Burgering, B. M., and Coffer, P. J. (1995) Protein kinase B (c-Akt) in phosphatidylinositol 3-OH kinase signal transduction. *Nature* **376,** 599–602
50. Hobbs, R. M., Seandel, M., Falciatori, I., Rafii, S., and Pandolfi, P. P. (2010) Plzf regulates germline progenitor self-renewal by opposing mTORC1. *Cell* **142,** 468–479
51. Hofmann, M. C. (2008) Gdnf signaling pathways within the mammalian spermatogonial stem cell niche. *Mol. Cell. Endocrinol.* **288,** 95–103
52. Lee, J., and Shinohara, T. (2011) Epigenetic modifications and self-renewal regulation of mouse germline stem cells. *Cell Res,* **21,** 1164–1171